BENCHMARK PID 2018

# Benchmark for PID control of Refrigeration Systems based on Vapour Compression

G. Bejarano, J. A. Alfaya, D. Rodríguez, M. G. Ortega
Departamento de Ingeniería de Sistemas y Automática. Escuela Técnica Superior de Ingeniería.
Universidad de Sevilla.
Camino de los Descubrimientos, s/n. 41092-Seville (Spain)
{gbejarano, jalonso9, drgarcia, mortega}@us.es

F. Morilla
Departamento de Informática y Automática
Escuela Técnica Superior de Ingeniería Informática. UNED.
C/. Juan del Rosal 16, 28040-Madrid (Spain)
fmorilla@dia.uned.es

## 1. INTRODUCTION

Refrigeration based on vapour compression is the leading technology worldwide in cooling generation, including air conditioning, refrigeration, and freezing. Controlling room temperature is involved in as widely diverse areas as human comfort, food storage and transportation, and industrial processes. Therefore, the applications of vapour-compression refrigeration systems are extensive: domestic, commercial, and industrial refrigeration, whose power range varies from less than 1 kW to above 1 MW [Rasmussen *et al.*, 2005]. Although in some cases air conditioning and refrigeration are separately considered, all these systems work the same way: they use the inverse Rankine cycle to remove heat from a cold reservoir (i.e. a cold storage room) and transfer it to a hot reservoir, normally the surroundings. A great deal of energy is required in such tasks, in both developing and developed countries, that affects negatively energy and economic balances [Buzelin *et al.*, 2005]. It is reported that approximately 30% of total energy over the world is consumed by Heating, Ventilating, and Air Conditioning (HVAC) processes, as well as refrigerators and water heaters [Jahangeer *et al.*, 2011], while the most recent Residential Energy Consumption Survey (RECS) shows that air conditioners and refrigerators represent 28% of home energy consumption in the United States [US Energy Information Administration, 2009]. Furthermore, supermarkets and department stores are known to be one of the largest consumers in the energy field, since official reports estimate that the average energy intensity for grocery stores is around 500 kWh/m$^2$ a year in USA, which means more than twice the energy consumed by a hotel or an office building per square meter [US Environmental Protection Agency, 2009]. It is stated that a medium-sized supermarket consumes up to 3 million kWh a year [Baxter, 2002], and around 60% of this great energy consumption is related to refrigeration systems [Suzuki *et al.*, 2011]. Considering commercial and residential buildings, around 45% of total electricity consumption is devoted to HVAC systems [Pérez-Lombard *et al.*, 2008; Kalkan *et al.*, 2012}.

Refrigeration systems are, as generally known, closed cycles, whose components are connected through various pipes and valves, which causes strong nonlinearities and high coupling. This is why the dynamic modelling of vapour-compression refrigeration systems is not definitely trivial matter. The most important elements regarding the dynamic modelling are the heat exchangers, while the expansion valve (EEV), the compressor, and the thermal behaviour of the secondary fluxes are statically modelled. The reason is that their dynamics are usually at least one order of magnitude faster than those of the evaporator and condenser.

Concerning control, there is an extensive literature related with control of refrigeration systems. To achieve high energy efficiency while satisfying the cooling demand, it must be taken into account that heat transfer at the evaporator is key for the overall efficiency. Heat transfer is widely recognized to be much higher when the refrigerant flow is two-phase. Thus, the highest evaporator efficiency would be achieved if the refrigerant at the evaporator outlet was saturated vapour. This ideal behaviour is not advisable nor applicable in practice, since the risk of liquid droplets appearing at the evaporator outlet is very high in transient, which must be definitely avoided because the evaporator outlet matches the compressor intake. Therefore, the approach conventionally applied in industry consists in operating the cycle with a certain degree of superheating of the refrigerant at the evaporator outlet ($T_{SH}$), which is held low to approximate to the ideal behaviour previously described. Therefore, the conventional control scheme is very simple: in addition to the reference imposed by the cooling demand, a low but constant set point on the degree of superheating $T_{SH}$ is applied and the controller is designed to get these two variables to track their references as efficiently as possible in presence of disturbances by manipulating the compressor speed and the expansion valve opening.

To design the tracking controller, it is important to take into account that the difficulty in controlling this process lies in high thermal inertia, dead times, high coupling between variables, and strong nonlinearities. The most used linear techniques which can be found in the literature are decentralized PID control [Underwood, 2001; Wang *et al.*, 2007; Marcinichen *et al.*, 2008; Salazar and Méndez, 2014], decoupling multivariable control [Shen *et al.*, 2010], LQG control [He, 1996; Schurt *et al.*, 2009-2010], model predictive control (MPC) [Razi *et al.*, 2006; Sarabia *et al.*, 2009; Ricker, 2010; Fallahsohi *et al.*, 2010], and robust $H_\infty$ control [Larsen and Holm, 2003, Bejarano *et al.*, 2015]. The main advantage of using PID controllers is their ease of implementation and tuning, while the advantage of more advanced controllers is mainly their performance improvement.

The Benchmark PID 2018 allows researchers to approach an important control problem in order to test their recent developments in the design of PID controllers. This document is organized as follows. The Refrigeration System and its control are presented in Section 2. The attention is first focused on the most general problem and then the MIMO problem selected for the Benchmark PID 2018 is addressed. Also, some details about the dynamic modelling of vapour compression refrigeration systems are given. Sections 3 and 4 describe how the test and comparative evaluation of multivariable PID controllers are carried out. All the examples mentioned in this document can be checked by uploading the files provided by the authors in the website: http://www.dia.uned.es/~fmorilla/benchmarkPID2018/. You can get also full documentation about the Benchmark PID 2018 in the website, including the appendix to this document entitled *The MATLAB & Simulink files to approach the Refrigeration System Control Problem*.

## 2. THE CONTROL OF REFRIGERATION SYSTEMS

A canonical one-compression-stage, one-load-demand refrigeration cycle is shown in Fig. 1, where the main components (the expansion valve, the compressor, the evaporator, and the condenser) are represented. Due to the growth of the electronics field, variable speed compressors and electronic expansion valves have gradually replaced older single speed compressors and thermostatic expansion valves, respectively. Such new components allow the development of smarter control strategies, not only to save energy but also to reduce fluctuations in the controlled variables and therefore achieve a more accurate control. The objective of the cycle is to remove heat from the secondary flux at the evaporator and reject heat at the condenser by transferring it to the secondary flux. The inverse Rankine cycle is applied, where the refrigerant enters the evaporator at low temperature and pressure and it evaporates while removing heat from the evaporator secondary flux. Then, the compressor increases the refrigerant pressure and temperature and it enters the condenser, where first its temperature decreases, secondly it condenses and finally it may become subcooled liquid while transferring heat to the condenser secondary flux. The expansion valve closes the cycle by upholding the pressure difference between the condenser and the evaporator.

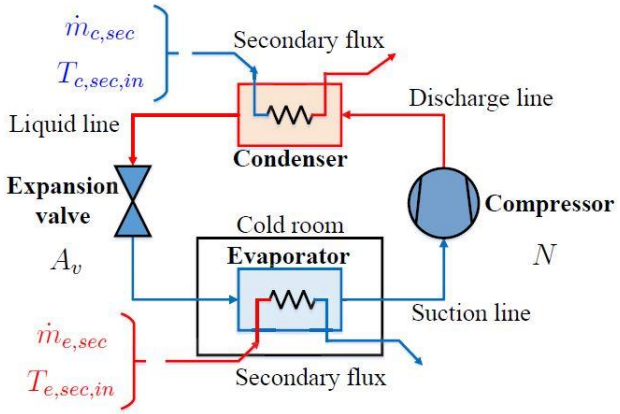


Fig. 1. Schematic picture of one-compression-stage, one-load-demand vapour- compression refrigeration cycle.

The main control objective is to provide the desired cooling power $\dot{Q}_e$. Furthermore, the generation of this cooling power is intended to be as efficient as possible, which implies controlling the degree of superheating $T_{SH}$. As widely known, energy efficiency is usually described in refrigeration field using the Coefficient of Performance ($COP$), which is defined as the ratio between the cooling power generated at the evaporator $\dot{Q}_e$ and the mechanical power provided by the compressor $\dot{W}_{comp}$, as indicated in Equation 1.1. Considering a one-compression-stage, one-load-demand cycle, the refrigerant mass flow $\dot{m}$ is the same at both components, thus the $COP$ turns out to depend only on intensive variables, specifically the characteristic enthalpies of the cycle, which are represented in the generic pressure-specific enthalpy chart (P-h diagram) shown in Fig. 2. Note that the blue dashed line related to the cooling level simply represents the refrigerant saturation pressure at the inlet temperature of the evaporator secondary flux $T_{e,sec,in}$. Similarly, the red dashed line related to the ambient refers to the refrigerant saturation pressure at the

inlet temperature of the condenser secondary flux $T_{c,sec,in}$. They have been included in the P-h diagram only to represent qualitatively the sign of the temperature difference between the refrigerant and the secondary flux at both heat exchangers.

$$COP = \frac{\dot{Q}_e}{\dot{W}_{comp}} = \frac{\dot{m}(h_{e,out} - h_{e,in})}{\dot{m}(h_{c,in} - h_{e,out})} = \frac{h_{e,out} - h_{e,in}}{h_{c,in} - h_{e,out}} \quad (1)$$

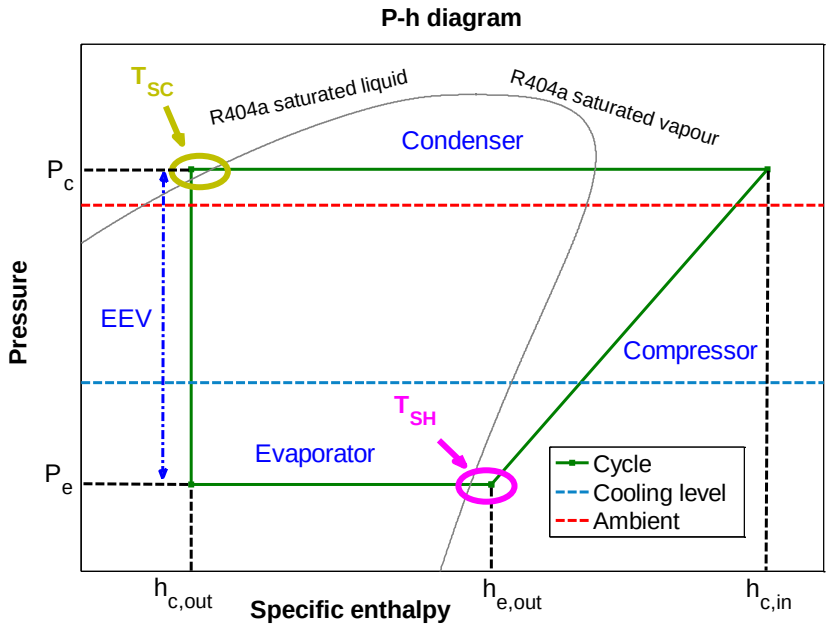


Fig. 2. P-h diagram of a one-compression-stage, one-load-demand vapour-compression cycle.

In the Benchmark PID 2018 a particular application of refrigeration systems is considered. The cycle, working with R404a as refrigerant, is expected to provide a certain cooling power $\dot{Q}_e$ to a continuous flow entering the evaporator as secondary flux. The evaporator secondary fluid is a 60% propylene glycol aqueous solution, whereas the condenser secondary fluid is air. Neither the mass flow $\dot{m}_{e,sec}$ nor the inlet temperature $T_{e,sec,in}$ of the evaporator secondary flux are intended to be controlled. Therefore, the cooling demand can be expressed as a reference on the outlet temperature of the evaporator secondary flux $T_{e,sec,out}$, where the mass flow and inlet temperature act as measurable disturbances. Regarding the condenser, the inlet temperature $T_{c,sec,in}$ and mass flow $\dot{m}_{c,sec}$ of the secondary flux are also considered as disturbances. The manipulated variables are the compressor speed $N$ and the expansion valve opening $A_v$.

The system block is represented in Fig. 3, where the manipulated variables, the controlled variables, and the disturbances are indicated. Two variables (the outlet temperature of the evaporator secondary flux $T_{e,sec,out}$ and the degree of superheating $T_{SH}$) are to be controlled by manipulating two variables (the compressor speed $N$ and the expansion valve opening $A_v$), considering also the disturbances, which are included in Table 1. The Coefficient of Performance $COP$ is used as quality steady-state performance variable.

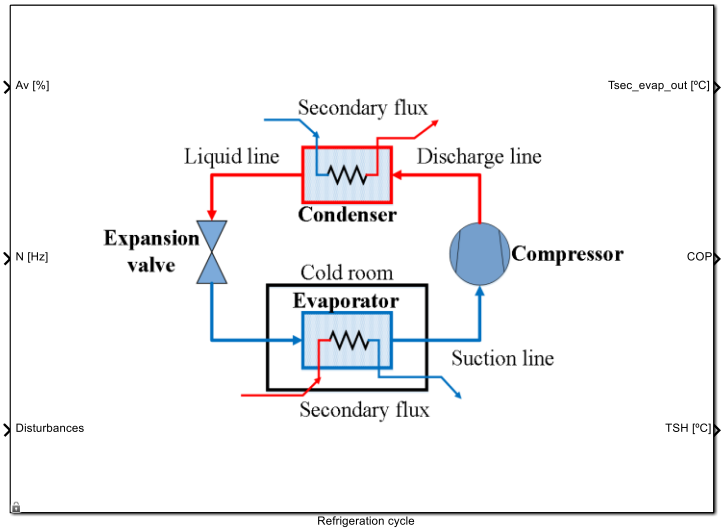


Fig. 3. Simulink block describing the vapour-compression refrigeration process.

| Disturbance | Mathematical symbol | Units |
|---|---|---|
| Inlet temperature of the condenser secondary flux | $T_{c,sec,in}$ | ºC |
| Mass flow of the condenser secondary flux | $\dot{m}_{c,sec}$ | g $s^{-1}$ |
| Inlet pressure of the condenser secondary flux | $P_{c,sec,in}$ | bar |
| Inlet temperature of the evaporator secondary flux | $T_{e,sec,in}$ | ºC |
| Mass flow of the evaporator secondary flux | $\dot{m}_{e,sec}$ | g $s^{-1}$ |
| Inlet pressure of the evaporator secondary flux | $P_{e,sec,in}$ | bar |
| Compressor surroundings temperature | $T_{surr}$ | ºC |

Table 1. Disturbance vector.

The Benchmark PID 2018 provides the Simulink model of Fig. 4 to test a multivariable discrete controller with or without feedforward. Nevertheless, any type of controller could be tested using this Simulink model.

### *2.1 About the controller*

The multivariable controller needs to be an 11x2 Simulink block, but it could be a continuous, a discrete, or a hybrid block. There is also total freedom to decide the structure of the block; the controller can use the eleven input signals or some of them. The eleven input signals are: the outlet temperature of the evaporator secondary flux (*Tsec_evap_out*), its reference (*Ref Tsec_evap_out*), the degree of superheating (*TSH*), its reference (*Ref TSH*), and the disturbance vector made up of seven variables. The two output signals (manipulated variables) are the valve opening (*Av*) and the compressor speed (*N*). Fig. 5 shows the multivariable controller included by default in the Benchmark PID 2018. It is a discrete decentralized controller, with a sample time of 1 second, where the outlet temperature of the evaporator secondary flux is controlled by means of the expansion valve, while the compressor speed controls the degree of superheating. The disturbance information is not used, thus it is a MIMO controller without feedforward compensation.

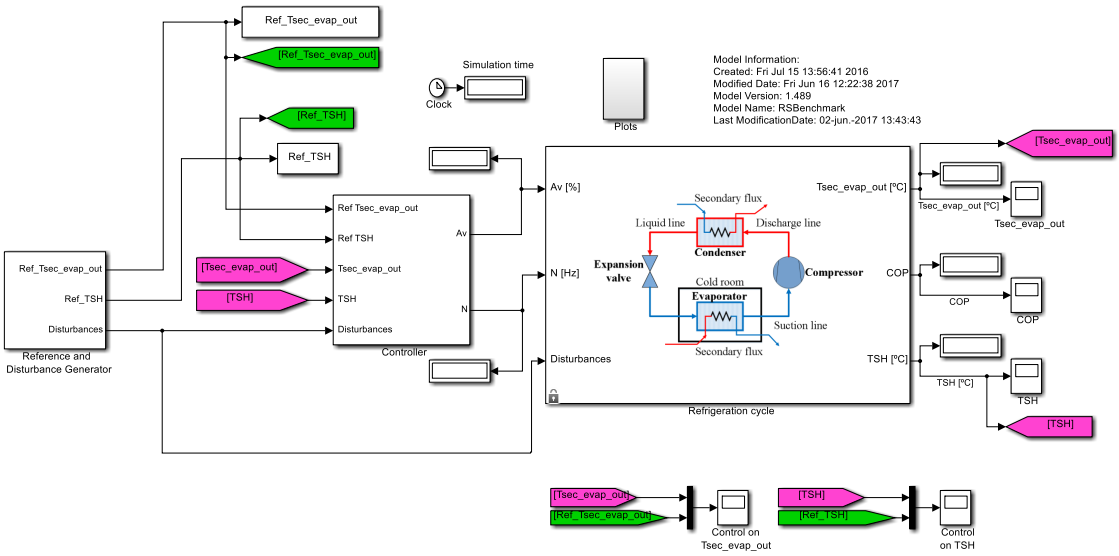


Fig. 4. Refrigeration Control System.

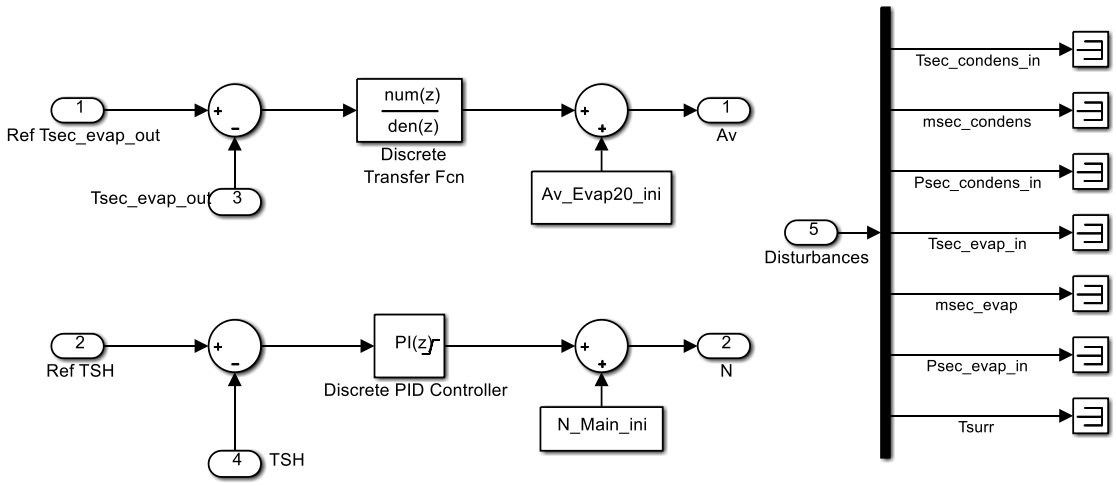


Fig. 5. The discrete decentralized controller included by default in the Refrigeration Control System.

| **Controller** | **Transfer function** |
|---|---|
| $T_{e,sec,out} - A_v$ | $\frac{-1.0136 - 0.0626z^{-1} + 0.9988z^{-2}}{1 - 1.9853z^{-1} + 0.9853z^{-2}}$ |
| $T_{SH} - N$ | $\frac{0.42 - 0.02z^{-1}}{1 - z^{-1}}$ |

Table 2. Discrete transfer functions used within the default controller.

*2.2 About the Vapour-Compression Refrigeration System Model*

It is stated in the Introduction that the most important elements regarding the dynamic modelling are the heat exchangers, while the expansion valve, the compressor, and the thermal behaviour of the secondary fluxes are statically modelled. The reason is that their dynamics are usually at least one order of magnitude faster than those of the evaporator and condenser.

A very detailed model of a heat exchanger is based on mass, energy, and momentum balances of the refrigerant, the secondary flux, and the material separating them that comprises the heat exchanger itself. This approach, dating to MacArthur *et al.* (1983), involves spatially discretizing the heat exchanger into an arbitrary number of control volumes, and thus leading to a numerical solution of a set of differential equations discretized into a finite difference form. The *finite-volume* (FV) approach provides very detailed knowledge about the system statics and dynamics, but due to its computational cost and complexity, it is inappropriate for model-based control strategies.

A simpler model with better balance between accuracy and computational cost may be obtained using the *moving-boundary* (MB) approach. This methodology divides the heat exchanger into a number of zones corresponding to different refrigerant states: superheated vapour, two-phase fluid, and/or subcooled liquid. Mass and energy balances are applied to each zone and, taking into account theses balances as well as other system constraints, the refrigerant variables at the heat exchanger outlet are obtained. The zone lengths are state variables, since they can vary with time depending on inputs and disturbances. A step further is developed by McKinley and Alleyne (2008): some control volumes are allowed to completely disappear and reappear without simulation issues, giving rise to the *switched moving boundary* (SMB) model. Different representations of the heat exchanger model, also known as *modes*, are defined depending on the existence or absence of each zone. For example, in the case of the evaporator, two *modes* are defined depending on the amount of superheated vapour, as represented in Fig. 6. In the case of the condenser, up to five different *modes* are considered, which are graphically described in Fig. 7. This model is validated and extended to startup and shutdown processes by Li and Alleyne (2010). The complexity, computational load, and accuracy of the SMB model have been recently compared to those of the FV formulation [Pangborn *et al.*, 2015]. It has been concluded that while the SMB approach can execute much more quickly in simulation than the FV approach, there is little difference in the achievable accuracy with respect to experimental data.

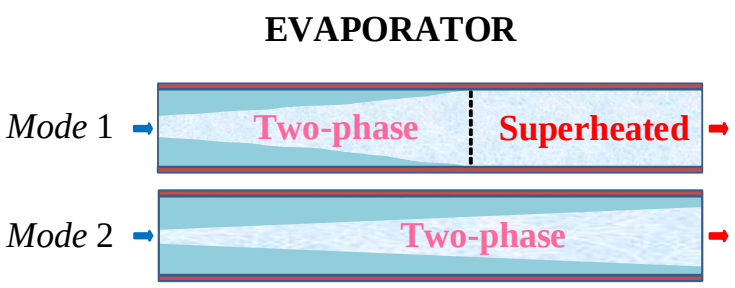


Fig. 6. Evaporator *modes* according to Li and Alleyne (2010)

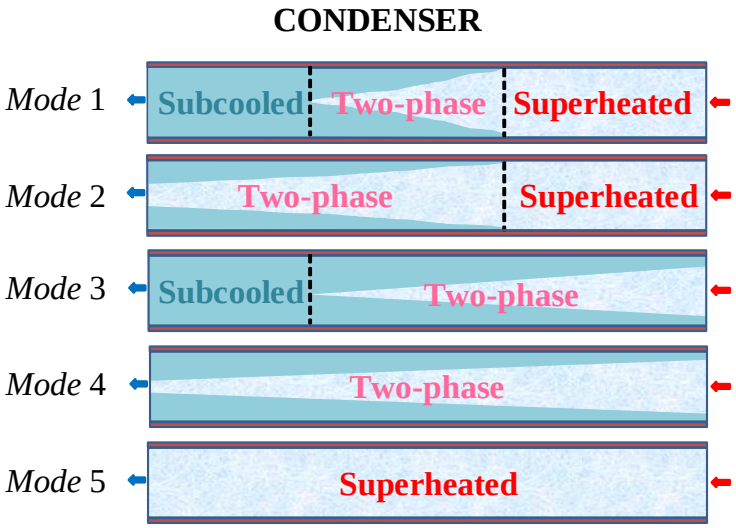


Fig. 7. Condenser *modes* according to Li and Alleyne (2010)

In addition to the FV and MB approaches, black-box models can be found in the literature. For instance, a neural network approach to identification of a heat exchanger is proposed by Bittanti and Piroddi (1997), while a simplified black-box model is proposed by Romero *et al.* (2011) to predict accurately the chilled water temperature dynamic response of a vapour-compression chiller, where the Box-Jenkins structure gets the best fit to experimental results. This modelling approach is suitable for control purposes, but only the identified output variables can be controlled.

In the Benchmark PID 2018 the SMB approach has been selected to model the refrigerant behaviour when circulating through the heat exchangers, due to its ability to adapt to different systems and its better trade-off between accuracy and computational load. Nevertheless, some considerations have been taken into account in order to reduce the model order of the original SMB model [McKinley and Alleyne, 2008; Li and Alleyne, 2010] and therefore its complexity.

Firstly, progressive replacement of environment-unfriendly refrigerants and rising costs of raw material have motivated changes in evaporator design, seeking low internal volume [Rasmussen and Larsen, 2011]; micro channel and plate heat exchangers are some examples of this trend. As a result, the evaporator dynamics become faster and, if compared to typical condenser dominant time constant, they can be disregarded without too much inaccuracy, thus the evaporator may be statically modelled and the condenser dynamics are considered as dominant.

Secondly, the refrigerant mass flow equilibrium between the condenser inlet and outlet is very fast compared to the heat transfer dominant dynamics, therefore a unique refrigerant mass flow passing through the condenser might be assumed, disregarding the fast transient due to mass flow imbalance.

Considering all these simplifications, the state vector of the whole cycle is reduced to that of the condenser. Moreover, when the condenser works in *mode* 1, the intrinsic dynamics of the state variables related to the superheated vapour zone and the two-phase zone have been disregarded due to density difference, which implies faster dynamics when

compared with the dominant dynamics related to the subcooled liquid zone. When the condenser works in *mode* 2, where the subcooled liquid zone is inactive, only the intrinsic dynamics of the state variables related to the superheated vapour zone have been disregarded, as well as the states related to the subcooled liquid zone.

The simplified SMB model has been developed in Simulink including constrained ranges for the inputs and outputs. Therefore, the following main features of the model are ensured:

1) It has a relatively low complexity while faithfully capturing the essential plant dynamics and its nonlinearities over a wide operating range.
2) The model is control-oriented in that the manipulated variables, the controlled variables, and the significant disturbances are explicitly shown.
3) The model is realistic since constraints on the manipulated variables are considered.

Some works have been published regarding the modelling, identification, optimization, and control of vapour-compression refrigeration systems by the authors of the Benchmark PID 2018. The corresponding references have been included at the end of this document for the keen reader [Rodríguez *et al.*, 2017, Bejarano *et al.*, 2017, Ruz *et al.*, 2017, Bejarano *et al.*, 2016, Rodríguez *et al.*, 2016, Alfaya *et al.*, 2015a-2015b]. Furthermore, it is important to remark that all fluid thermodynamic properties are computed in the Benchmark PID 2018 using the *CoolProp* tool [Bell *et al.*, 2014].

Table 3 includes the ranges of the input variables accepted by the system block shown in Fig. 3. It is important to note that the manipulated variables $A_v$ and $N$ are saturated within the system block, in such a way that if a value out of the ranges indicated in Table 3 is applied to the block, it will be saturated to the nearest value within the corresponding range. Note also that the influence of the inlet pressures of the secondary fluxes have not been studied, since their values only affect the calculation of the thermodynamic properties and they are not expected to change appreciably in a real application.

| **Input variable** | | **Range** | **Units** |
|---|---|---|---|
| Manipulated variables | $A_v$ | [10 – 100] | % |
| | $N$ | [30 - 50] | Hz |
| Disturbances | $T_{c,sec,in}$ | [27 – 33] | ºC |
| | $\dot{m}_{c,sec}$ | [125 – 175] | g $s^{-1}$ |
| | $P_{c,sec,in}$ | – | bar |
| | $T_{e,sec,in}$ | [-22 – -18] | ºC |
| | $\dot{m}_{e,sec}$ | [0.055 – 0.0075] | g $s^{-1}$ |
| | $P_{e,sec,in}$ | – | bar |
| | $T_{surr}$ | [20 – 30] | ºC |

Table 3. Input variable ranges.

The model is ready to be controlled with a sampling period equal or greater than 1 second, starting always at the same operating point given by the variables indicated in Table 4.

| Variable | | Value | Units |
|---|---|---|---|
| Manipulated variables | $A_v$ | ≅ 48.79 | % |
| | $N$ | ≅ 36.45 | Hz |
| Disturbances | $T_{c,sec,in}$ | 30 | ºC |
| | $\dot{m}_{c,sec}$ | 150 | g $s^{-1}$ |
| | $P_{c,sec,in}$ | 1 | bar |
| | $T_{e,sec,in}$ | -20 | ºC |
| | $\dot{m}_{e,sec}$ | 64.503 | g $s^{-1}$ |
| | $P_{e,sec,in}$ | 1 | bar |
| | $T_{surr}$ | 25 | ºC |
| Output variables | $T_{e,sec,out}$ | ≅ -22.15 | ºC |
| | $T_{SH}$ | ≅ 14.65 | ºC |

Table 4. Initial operating point.

## 3. TESTING MULTIVARIABLE CONTROLLERS

The Refrigeration Control System of Fig. 4 is ready to test any multivariable controller operating the system. The MATLAB program *RS_simulation_management.m* is provided to help this test. It is necessary to define the simulation time and the sample time, as well as a name for the data file generated when the simulation ends. An example name using the date, hour, and minute when the simulation is started is proposed, but the simulation data can be logged as the user wishes. The mentioned MATLAB program also automates the simulation execution, data logging, and relevant data representation.

A standard simulation, starting from the operating point described in Table 4, has been scheduled for the Benchmark PID 2018. The simulation, see Fig. 8-9, includes step changes in the references on $T_{e,sec,out}$ and $T_{SH}$, and in the most important disturbances: the inlet temperature of the evaporator secondary flux $T_{e,sec,in}$ and the inlet temperature of the condenser secondary flux $T_{c,sec,in}$.

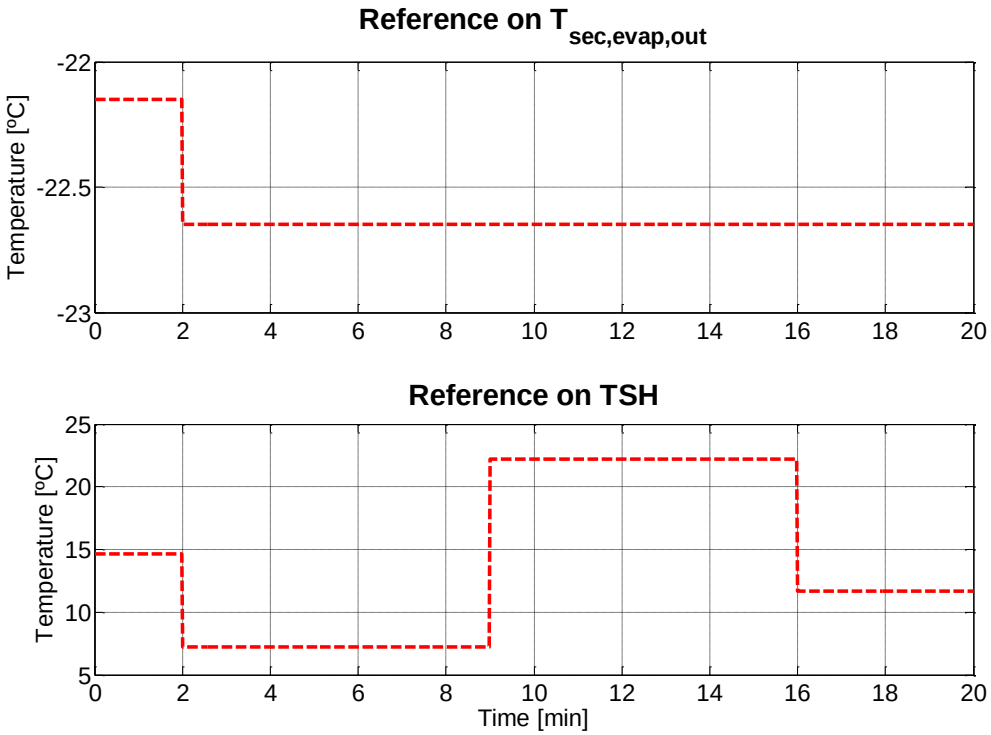


Fig. 8. The standard simulation for Benchmark PID 2018 generates changes in the references $T_{e,sec,out}$ and $T_{SH}$.

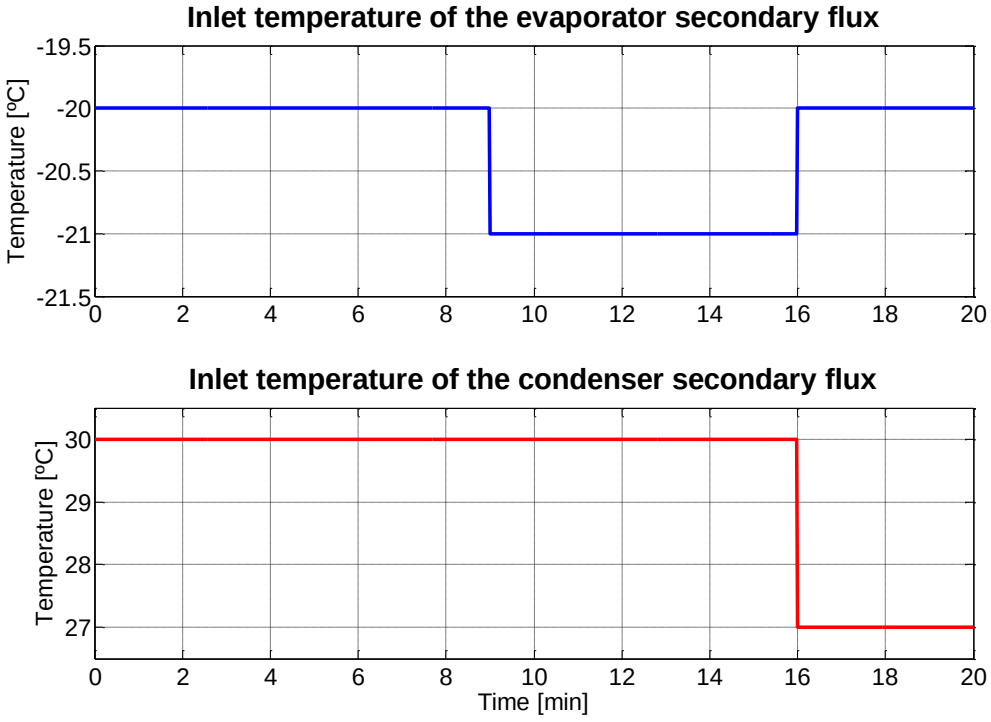


Fig. 9. The standard simulation for Benchmark PID 2018 generates changes in two disturbances: $T_{e,sec,in}$ and $T_{c,sec,in}$.

It is observed in Fig. 8 that, although the reference on $T_{e,sec,out}$ does not vary from minute 2 of the simulation, the references on $T_{SH}$ are changed when applying changes in the disturbances. It is a special feature of the refrigeration systems, which is not exactly a

MIMO process with independent variables. Fig. 10 shows a variety of steady-state points in the space of the controlled variables. These points have been obtained imposing values all over the range of the manipulated variables, and considering three different values of one of the disturbances, specifically $T_{c,sec,in}$. It is observed in Fig. 10 that for a given desired value of $T_{e,sec,out}$, there exists a specific range of achievable $T_{SH}$, thus the reference on the degree of superheating cannot be set regardless of the reference on $T_{e,sec,out}$. Furthermore, the range of achievable $T_{SH}$ is expected to vary for different values of the disturbances; this is why the reference on $T_{SH}$ is not only altered when varying the reference on $T_{e,sec,out}$, but also when the disturbances are modified.

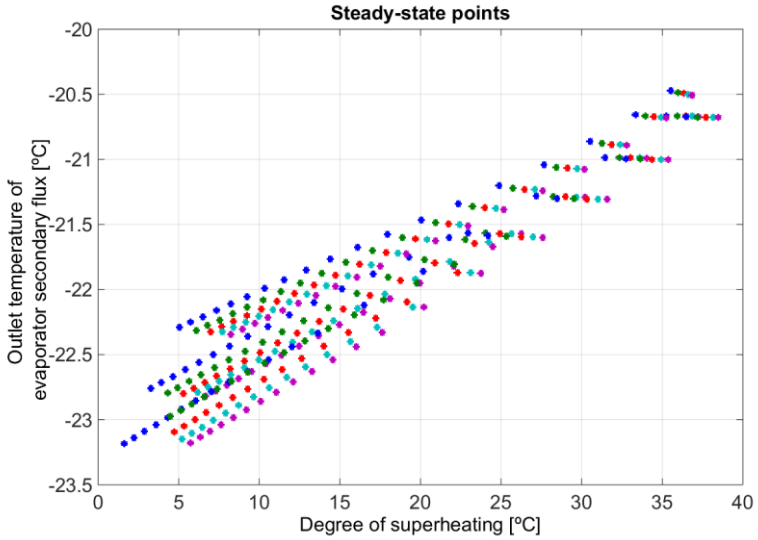


Fig. 10. Steady-state map in the space of the controlled variables, for three values within the range considered for $T_{c,sec,in}$

This simulation or any other scheduled simulations can be used to explore the refrigeration system operating points, always according to the input variable ranges expressed in Table 3. Fig. 11-16 show the results of the standard simulation using the default controller described in Section 2.1. The MATLAB program *RS_simulation_management.m* generates some figures where the controlled variables and the manipulated ones are represented. Moreover, some other interesting cycle variables are shown, such as the refrigerant pressures, thermal powers, refrigerant mass flow, and the $COP$, among others.

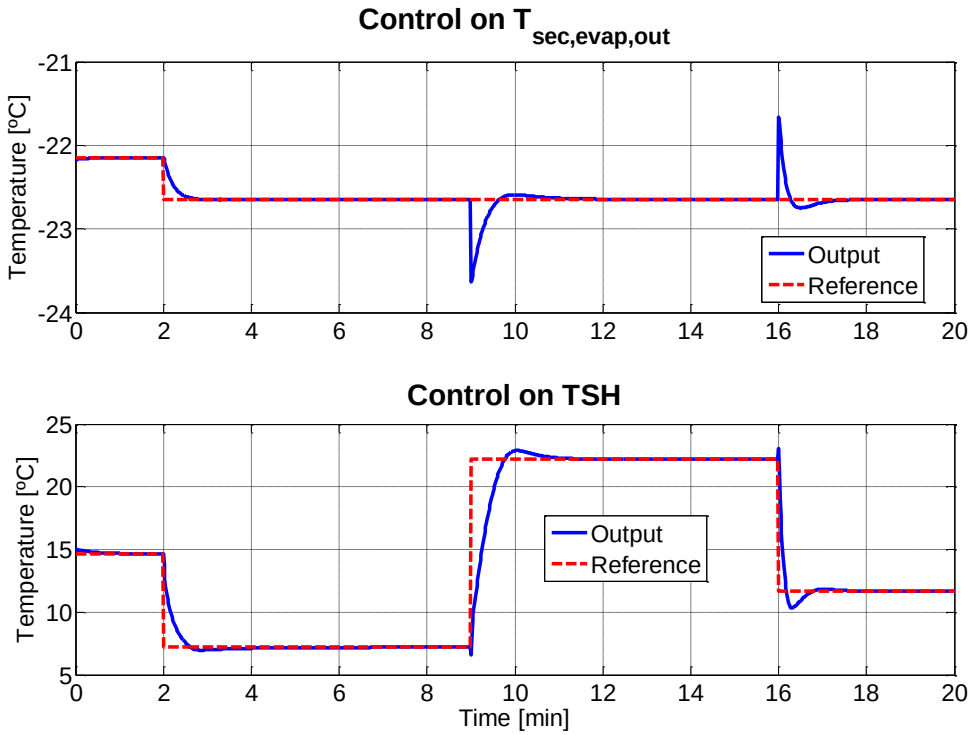


Fig. 11. Example of the standard simulation with the MIMO Refrigeration Control System. Controlled variables.

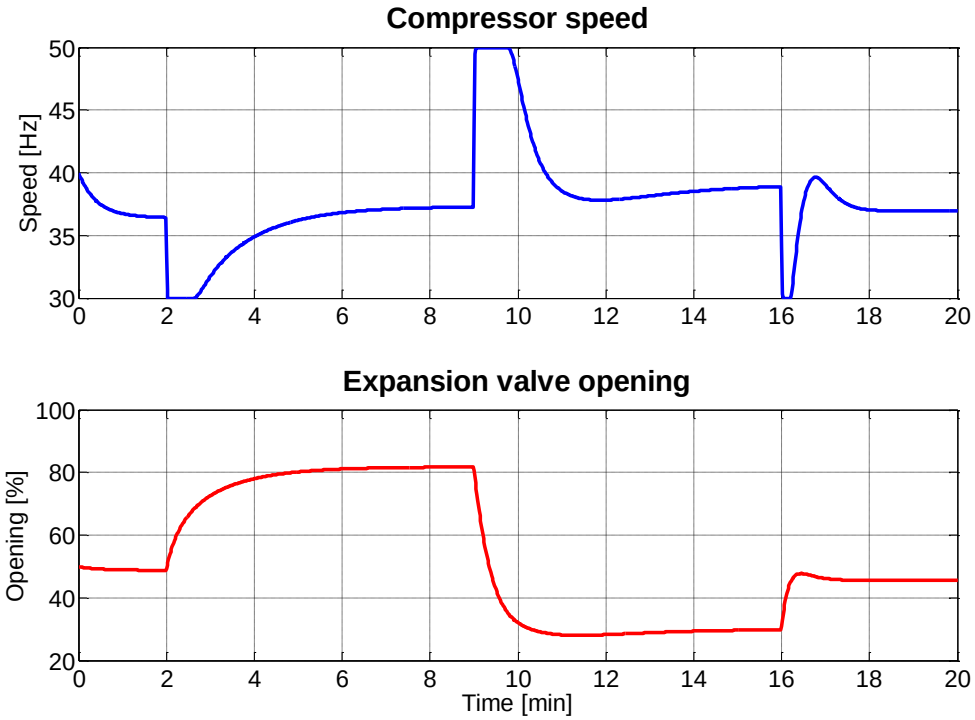


Fig. 12. Example of the standard simulation with the MIMO Refrigeration Control System. Manipulated variables.

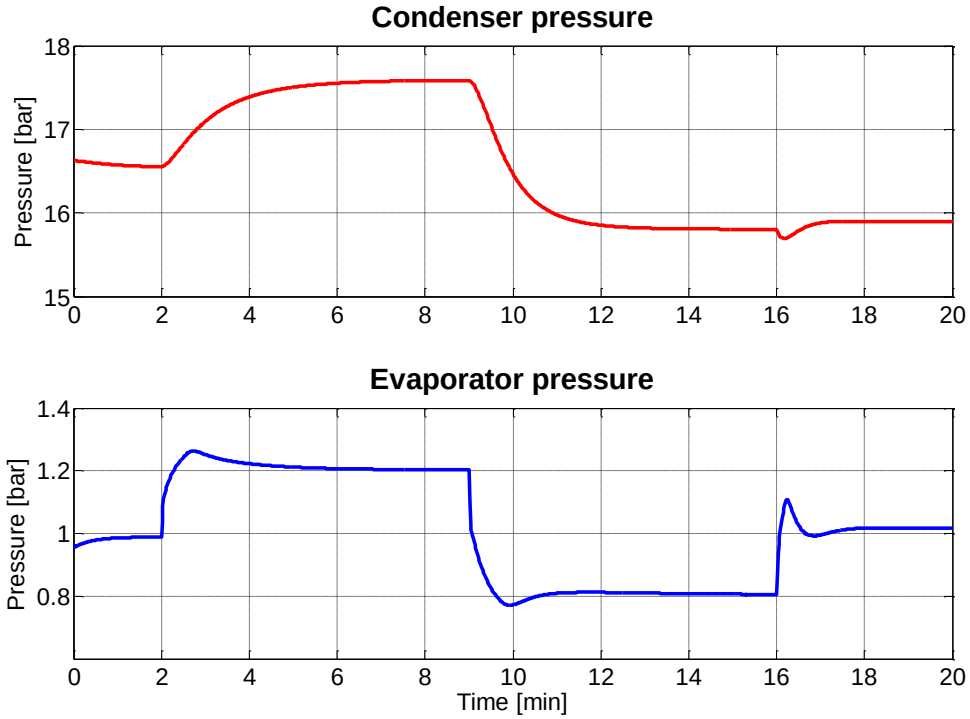


Fig. 13. Example of the standard simulation with the MIMO Refrigeration Control System. Evaporation and condensation pressures.

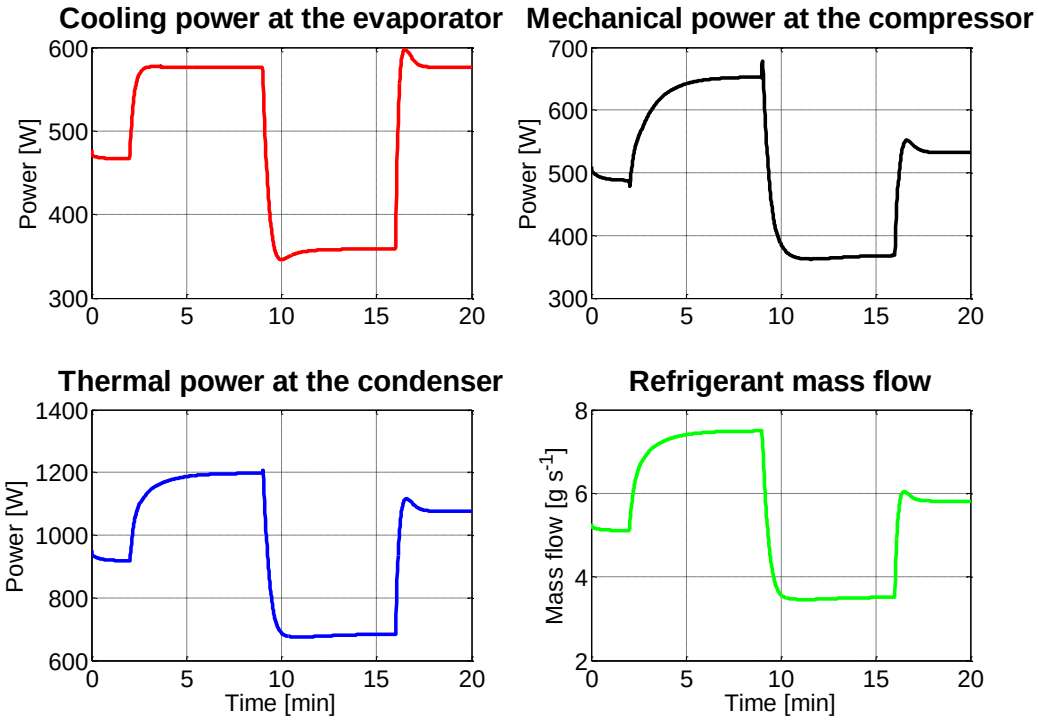


Fig. 14. Example of the standard simulation with the MIMO Refrigeration Control System. Thermal power at each component and refrigerant mass flow.

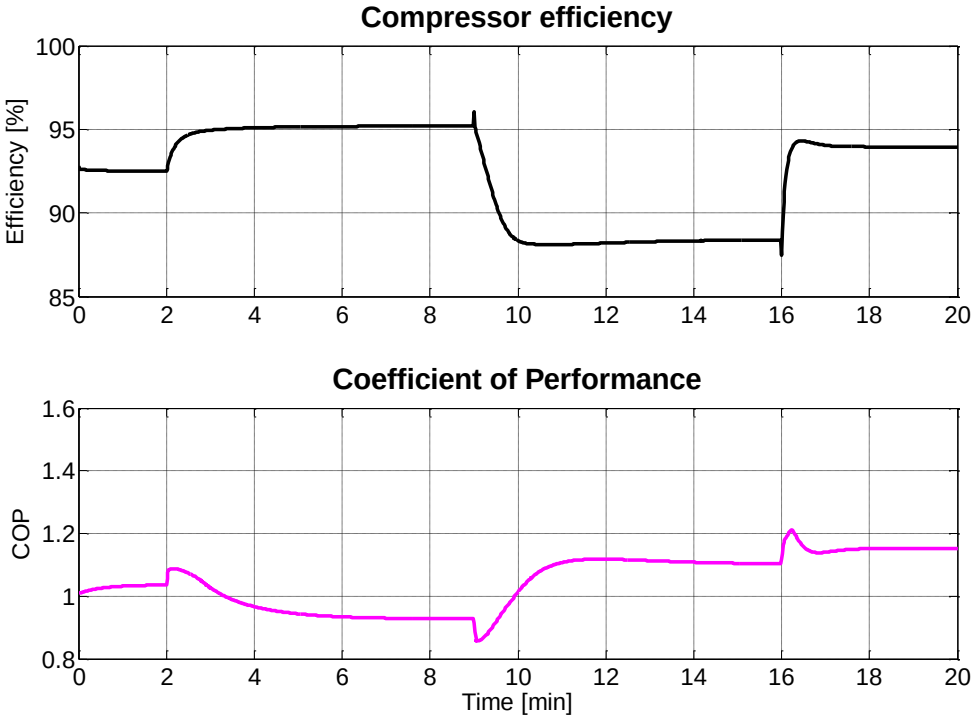


Fig. 15. Example of the standard simulation with the MIMO Refrigeration Control System. Compressor efficiency and Coefficient of Performance.

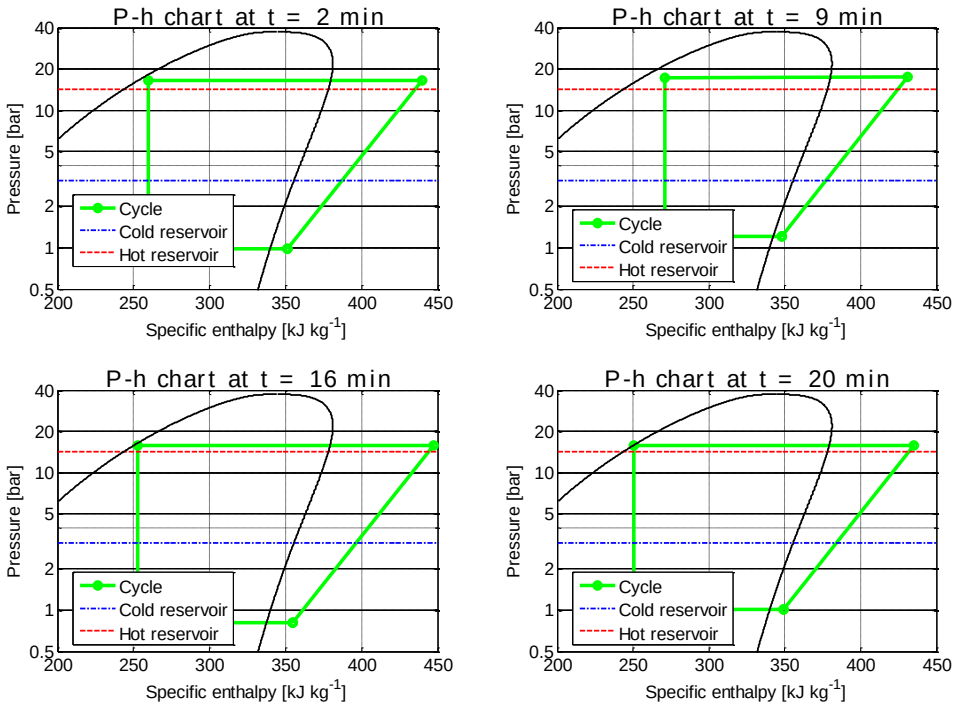


Fig. 16. Example of the standard simulation with the MIMO Refrigeration Control System. P-h charts at different simulation instants.

Note in Fig. 14 that the increase in the cooling power when applying the downward step on $T_{e,sec,out}$ (minute 2 of the simulation) involves around 25% higher power, despite the change in $T_{e,sec,out}$ being small (0.5 ºC).

**Remark 1**: The example of the standard simulation presented in this section was saved in the data file *RSBenchmark_20170524_13_48.mat*. Its results can be displayed by loading that file and calling the MATLAB function *data_representation.p*.

## 4. COMPARING MULTIVARIABLE CONTROLLERS

The Benchmark PID 2018 also facilitates the qualitative and quantitative comparison of two controllers based on the same simulation. Fig. 17-18 are an example of the qualitative comparison. A multivariable PID controller is compared with the default controller described in Section 2. The latter is labelled as *Controller 1* in the figures, while the multivariable PID controller is *Controller 2*. This example can be checked by calling the MATLAB function *RS_qualitative_comparison.p* with the names of the two data files (for example *file1.mat* and *file2.mat*, where *file1.mat* regards to the default controller) as input arguments and without output arguments, as follows:

*RS_qualitative_comparison('file','file2')*

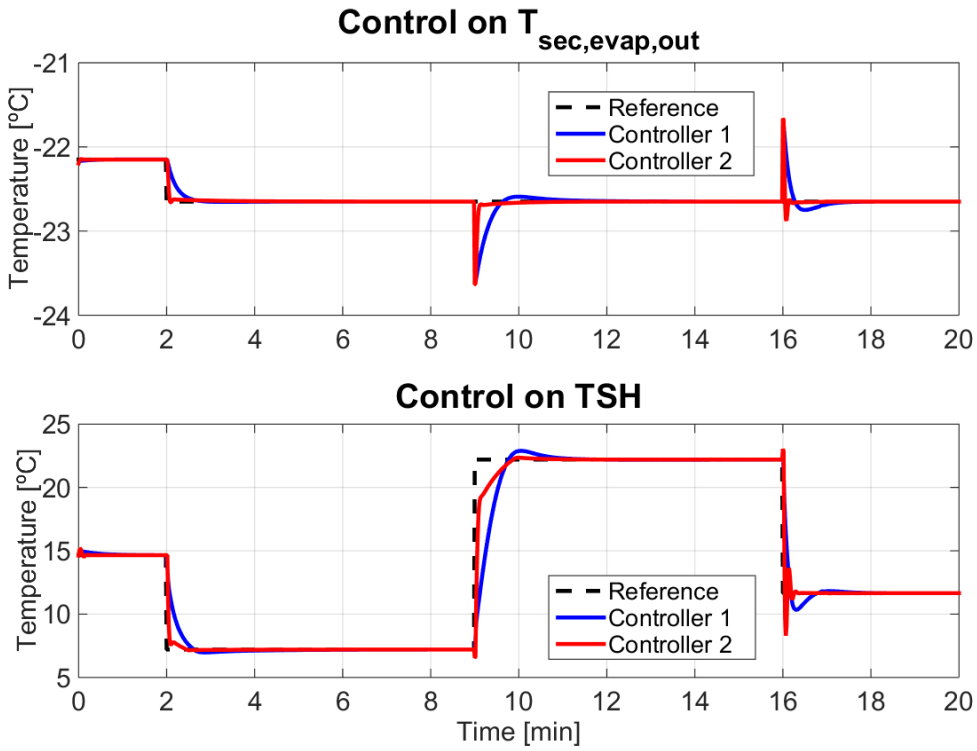


Fig. 17. Example of qualitative comparison of two standard simulations with the MIMO Refrigeration Control System. Controlled variables.

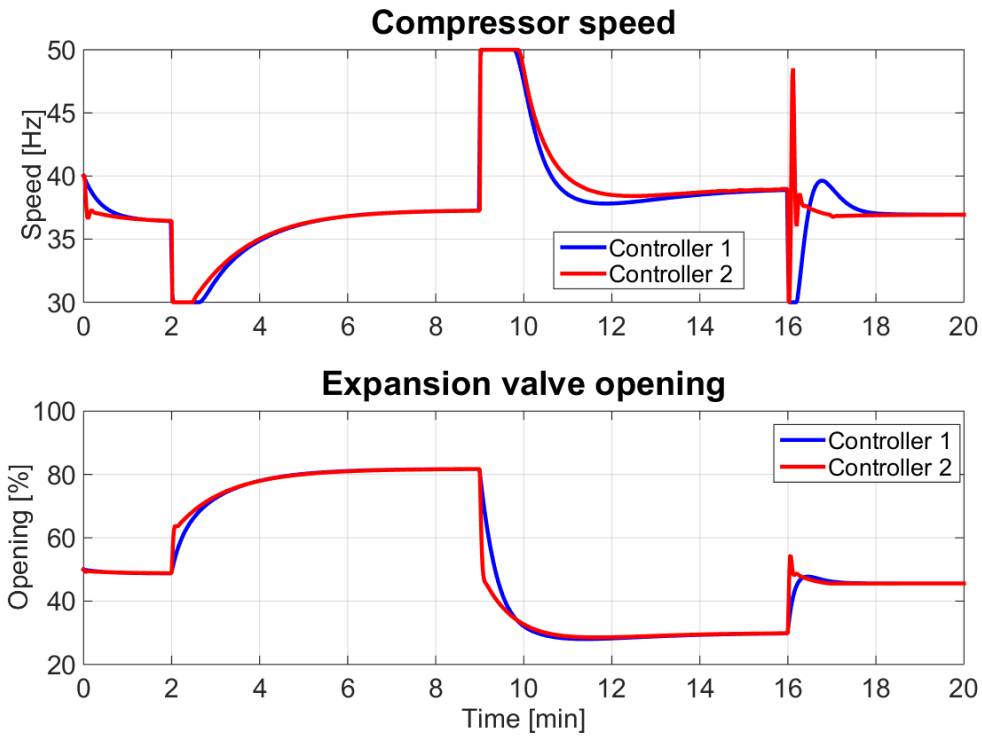


Fig. 18. Example of qualitative comparison of two standard simulations with the MIMO Refrigeration Control System. Manipulated variables.

The MATLAB function *RS_qualitative_comparison.p* also generates other comparative figures regarding the refrigerant pressures, the thermal powers, the refrigerant mass flow, and the performance indices, similar to Fig. 13-15.

In the quantitative comparison, one of them plays the role of controller of reference (for example the labelled *Controller 1* in Fig. 17-18) and the other one plays the role of controller to evaluate (for example the labelled *Controller 2* in Fig. 17-18). Eight individual performance indices and one combined index are evaluated in this comparison. The first two indices are the Ratios of Integrated Absolute Error (*RIAE*), taking into account that both the outlet temperature of evaporator secondary flux (*Tsec_evap_out*) and the degree of superheating (*TSH*) should follow their respective references. The third is the Ratio of Integrated Time multiplied Absolute Error (*RITAE*) for the first controlled variable (*Tsec_evap_out*), taking into account that the standard simulation only includes one sudden change in its reference. The fourth, fifth, and sixth indices are the Ratios of Integrated Time multiplied Absolute Error (*RITAE*) for the second controlled variable (*TSH*), taking into account that the standard simulation includes three sudden changes in its reference. The seventh and eighth indices are the Ratios of Integrated Absolute Variation of Control signal (*RIAVU*) for the two manipulated variables, the valve opening ($A_v$) and the compressor speed ($N$). The combined index is obtained as the mean value of the eight individual indices using a weighting factor for each index. The following expressions, which summarize these indices, have been programmed in the MATLAB function called *RS_quantitative_comparison.p*.

$$\mathrm{IAE}_i = \int_0^{\mathrm{time}} \left| e_i(t) \right| \, \mathrm{dt} \tag{2}$$

$$\mathrm{ITAE}_i = \int_{t_c}^{t_c+t_s} (t-t_c)\ |e_i(t)|\ dt \tag{3}$$

$$\mathrm{IAVU}_i = \int_0^{time} \left|\frac{d\,u_i(t)}{dt}\right| dt \tag{4}$$

$$\mathrm{RIAE}_i(C_2,C_1) = \frac{\mathrm{IAE}_i(C_2)}{\mathrm{IAE}_i(C_1)} \tag{5}$$

$$\mathrm{RITAE}_i(C_2,C_1,t_c,t_s) = \frac{\mathrm{ITAE}_i(C_2,t_c,t_s)}{\mathrm{ITAE}_i(C_1,t_c,t_s)} \tag{6}$$

$$\mathrm{RIAVU}_i(C_2,C_1) = \frac{\mathrm{IAVU}_i(C_2)}{\mathrm{IAVU}_i(C_1)} \tag{7}$$

$$J(C_2,C_1) = \frac{\begin{array}{l} w_1\ \mathrm{RIAE}_1(C_2,C_1) + w_2\ \mathrm{RIAE}_2(C_2,C_1) + w_3\ \mathrm{RITAE}_1(C_2,C_1,t_{c1},t_{s1}) \\ + w_4\ \mathrm{RITAE}_2(C_2,C_1,t_{c2},t_{s2}) + w_5\ \mathrm{RITAE}_2(C_2,C_1,t_{c3},t_{s3}) \\ + w_6\ \mathrm{RITAE}_2(C_2,C_1,t_{c4},t_{s4}) + w_7\ \mathrm{RIAVU}_1(C_2,C_1) + w_8\ \mathrm{RIAVU}_2(C_2,C_1) \end{array}}{\sum_1^8 w_i} \tag{8}$$

The example of Table 5 can be checked by calling the quantitative MATLAB function with the names of the data files *file1.mat* and *file2.mat*, where *file1.mat* regards to the controller of reference, as follows:

*[R_Indices, J] = RS_quantitative_comparison('file','file2')*

| Index | Value |
|---|---|
| $\mathrm{RIAE}_1(C_2,C_1)$ | 0.3511 |
| $\mathrm{RIAE}_2(C_2,C_1)$ | 0.4458 |
| $\mathrm{RITAE}_1(C_2,C_1,t_{c1},t_{s1})$ | 1.6104 |
| $\mathrm{RITAE}_2(C_2,C_1,t_{c2},t_{s2})$ | 0.1830 |
| $\mathrm{RITAE}_2(C_2,C_1,t_{c3},t_{s3})$ | 0.3196 |
| $\mathrm{RITAE}_2(C_2,C_1,t_{c4},t_{s4})$ | 0.1280 |
| $\mathrm{RIAVU}_1(C_2,C_1)$ | 1.1283 |
| $\mathrm{RIAVU}_2(C_2,C_1)$ | 1.3739 |
| $J(C_2,C_1)$ | 0.68209 |

Table 5. Relative indices and the combined index associated to the qualitative controller comparison represented in Fig. 17-18.

As shown in Fig. 17, *Controller 2* achieves tighter control on the outlet temperature of the evaporator secondary flux and the degree of superheating than *Controller 1*, specially regarding the disturbance rejection, which is reflected in almost all indices. However, the

control effort in *Controller 2* is higher, as shown in Fig. 18, thus relative indices $\mathrm{RIAVU}_1(C_2,C_1)$ and $\mathrm{RIAVU}_2(C_2,C_1)$ are greater than one. Considering the index weighting, the overall performance of *Controller 2* yields to a better combined index $J(C_2,C_1)$.

**Remark 2**: The qualitative and quantitative comparison presented in this section were carried out using the data files *RSBenchmark_20170524_13_48.mat* and *RSBenchmark_20170528_22_34.mat*.

ACKNOWLEDGEMENTS

The authors would like to acknowledge MCeI, Grant DPI2015-70973-R, for funding this work.

REFERENCES

B. P. Rasmussen, A. Musser, and A. G. Alleyne (2005), "Model-driven system identification of transcritical vapor compression systems," IEEE Trans. Control Syst. Technol., vol. 13, pp. 444–451.

L. O. S. Buzelin, S. C. Amico, J. V. C. Vargas, and J. A. R. Parise (2005), "Experimental development of an intelligent refrigeration system," Int. J. Refrig., vol. 28, no. 2, pp. 165–175.

K. A. Jahangeer, A. A. O. Tay, and M. R. Islam (2011), "Numerical investigation of transfer coefficients of an evaporatively-cooled condenser," Appl. Therm. Eng., vol. 31, no. 10, pp. 1655–1663.

US Energy Information Administration (2009), "Residential energy consumption survey (RECS)," Energy Information Administration, Washington D.C, USA, Tech. Rep.

US Environmental Protection Agency (2009), "National action plan for energy efficiency: Sector collaborative on energy efficiency accomplishments and next steps." http://www.epa.gov/cleanenergy/documents/suca/sector_collaborative.pdf

V. D. Baxter (2002), "Advances in supermarket refrigeration systems," Oak Ridge Natl. Lab., Oak Ridge, Tennessee 37831-6070.

Y. Suzuki, Y. Yamaguchi, K. Shiraishi, D. Narumi, and Y. Shimoda (2011), "Analysis and modeling of energy demand of retail stores," in 12th Conf. of Int. Build. Perform. Simul. Assoc.

L. Pérez-Lombard, J. Ortiz, and C. Pout (2008), "A review on buildings energy consumption information," Energy and Build., vol. 40, no. 3, pp. 394–398.

N. Kalkan, E. A. Young, and A. Celiktas (2012), "Solar thermal air conditioning technology reducing the footprint of solar thermal air conditioning," Renew. and Sustain. Energy Rev., vol. 16, no. 8, pp. 6352–6383.

C. P. Underwood (2001), "Analysing multivariable control of refrigeration plant using MATLAB/Simulink," in VII Int. IBPSA Conf., vol. 1, 2001, pp. 287–294.

J. Wang, C. Zhang, Y. Jing, and D. An (2007), "Study of neural network PID control in variable-frequency air-conditioning system," in IEEE Int. Conf. on Control and Autom., pp. 317–322.

J. Marcinichen, T. del Holanda, and C. Melo (2008), "A dual SISO controller for a vapor compression refrigeration system," in Int. Refrig. and Air Cond. Conf., vol. 2444.

M. Salazar and F. Méndez (2014), "PID control for a single-stage transcritical $CO_2$ refrigeration cycle," Appl. Therm. Eng., vol. 67, no. 1, pp. 429–438.

Y. Shen, W.-J. Cai, and S. Li, (2010) "Normalized decoupling control for high-dimensional MIMO processes for application in room temperature control HVAC systems," Control Eng. Pract., vol. 18, no. 6, pp. 652–664.

X.-D. He (1996), "Dynamic modeling and multivariable control of vapor compression cycles in air conditioning systems," Ph.D. dissertation, Massachusetts Institute of Technology, Massachusetts, USA.

L. C. Schurt, C. J. L. Hermes, and A. Trofino-Neto (2009), "A model-driven multivariable controller for vapor compression refrigeration systems," Int. J. of Refrig., vol. 32, no. 7, pp. 1672–1682.

L. C. Schurt, C. J. L. Hermes, and A. Trofino-Neto (2010), "Assessment of the controlling envelope of a model-based multivariable controller for vapor compression refrigeration systems," Appl. Therm. Eng., vol. 30, no. 13, pp. 1538–1546.

M. Razi, M. Farrokhi, M. Saeidi, and A. F. Khorasani (2006), "Neuro-predictive control for automotive air conditioning system," in Eng. of Intell. Syst., 2006 IEEE Int. Conf. on.

D. Sarabia, F. Capraro, L. F. Larsen, and C. de Prada (2009), "Hybrid NMPC of supermarket display cases," Control Eng. Pract., vol. 17, no. 4, pp. 428–441.

N. L. Ricker (2010), "Predictive hybrid control of the supermarket refrigeration benchmark process," Control Eng. Pract., vol. 18, no. 6, pp. 608–617.

H. Fallahsohi, C. Changenet, S. Placé, C. Ligeret, and X. Lin-Shi (2010), "Predictive functional control of an expansion valve for minimizing the superheat of an evaporator," Int. J. of Refrig., vol. 33, no. 2, pp. 409–418.

L. S. Larsen and J. R. Holm (2003), "Modelling and multi-variable control of refrigeration systems," ECOS 2003.

G. Bejarano, J. A. Alfaya, M. G. Ortega, and F. R. Rubio (2015), "Multivariable analysis and $H_\infty$ control of a one-stage refrigeration cycle," Appl. Therm. Eng., vol. 91, pp. 1156–1167.

J. W. MacArthur, G. D. Meixel, and L. S. Shen (1983), "Application of numerical methods for predicting energy transport in earth contact systems," Appl. Energy, vol. 13, no. 2, pp. 121–156.

T. L. McKinley and A. G. Alleyne (2008), "An advanced nonlinear switched heat exchanger model for vapor compression cycles using the moving-boundary method," Int. J. of Refrig., vol. 31, no. 7, pp. 1253–1264.

B. Li and A. G. Alleyne (2010), "A dynamic model of a vapor compression cycle with shut-down and start-up operations," Int. J. of Refrig., vol. 33, no. 3, pp. 538–552.

H. Pangborn, A. G. Alleyne, and N. Wu (2015), "A comparison between finite volume and switched moving boundary approaches for dynamic vapor compression system modeling," Int. J. of Refrig., vol. 53, pp. 101–114.

S. Bittanti and L. Piroddi (1997), "Nonlinear identification and control of a heat exchanger: a neural network approach," J. of the Frankl. Inst., vol. 334, no. 1, pp. 135 -153.

J. A. Romero, J. Navarro-Esbrí, and J. M. Belman-Flores (2011), "A simplified black-box model oriented to chilled water temperature control in a variable speed vapour compression system," Appl. Therm. Eng., vol. 31, no. 2, pp. 329–335.

H. Rasmussen and L. F. S. Larsen (2011), "Non-linear and adaptive control of a refrigeration system," IET Control Theory Appl., vol. 5, no. 2, pp. 365–378.

D. Rodríguez, G. Bejarano, J. A. Alfaya, M. G. Ortega, and F. Castaño (2017), "Parameter identification of a multi-stage, multi-load-demand experimental refrigeration plant," Control Eng. Pract., vol. 60, pp. 133–147.

G. Bejarano, J. A. Alfaya, M. G. Ortega, and M. Vargas (2017), "On the difficulty of globally optimally controlling refrigeration systems," Appl. Therm. Eng., vol. 111, pp. 1143–1157.

M. Ruz, J. Garrido, F. Vázquez, and F. Morilla (2017), "A hybrid modeling approach for steady-state optimal operation of vapor compression refrigeration cycles," Appl. Therm. Eng., vol. 120, pp. 74–87.

G. Bejarano, D. Rodríguez, J. A. Alfaya, M. G. Ortega, and F. Castaño (2016), "On identifying steady-state parameters of an experimental mechanical-compression refrigeration plant," Appl. Therm. Eng., vol. 109, pp. 318–333.

D. Rodríguez, J. A. Alfaya, G. Bejarano, M. G. Ortega, and F. Castaño (2016), "Steady-state parameter estimation of an experimental vapour compression refrigeration plant," in Eur. Control Conf. (ECC), Aalborg (Denmark). IEEE, pp. 43–48.

J. A. Alfaya, G. Bejarano, M. G. Ortega, and F. R. Rubio (2015a), "Controllability analysis and robust control of a one-stage refrigeration system," Eur. J. of Control, vol. 26, pp. 53–62.

J. A. Alfaya, G. Bejarano, M. G. Ortega, and F. R. Rubio (2015b), "Multi-operating-point robust control of a one-stage refrigeration cycle," in Eur. Control Conf. (ECC), Linz (Austria). IEEE, pp. 3490–3495.

I. H. Bell, J. Wronski, S. Quoilin, and V. Lemort (2014), "Pure and pseudo-pure fluid thermophysical property evaluation and the open-source thermophysical property library CoolProp," Ind. and Eng. Chem. Res., vol. 53, no. 6, pp. 2498–2508, www.coolprop.org